Title	A Novel Stator Doubly Fed Doubly Salient Permanent Magnet Brushless Machine
Author(s)	Chau, KT; Jiang, JZ; Wang, Y
Citation	Ieee Transactions On Magnetics, 2003, v. 39 n. 5 II, p. 3001-3003
Issued Date	2003
URL	http://hdl.handle.net/10722/42964
Rights	©2003 IEEE. Personal use of this material is permitted. However, permission to reprint/republish this material for advertising or promotional purposes or for creating new collective works for resale or redistribution to servers or lists, or to reuse any copyrighted component of this work in other works must be obtained from the IEEE.

A Novel Stator Doubly Fed Doubly Salient Permanent Magnet Brushless Machine

K. T. Chau, *Member, IEEE*, J. Z. Jiang, and Yong Wang, *Student Member, IEEE*

***Abstract*—A novel stator doubly fed doubly salient permanent magnet (PM) brushless machine is proposed. The novelty of this machine is to purposely add an extra flux path in shunt with each PM pole, hence amplifying the effect of flux weakening for constant power operation. Magnetic circuit analysis is adopted to illustrate the novelty. Machine flux paths and performance curves determined by a finite-element analysis are presented for various excitations. The corresponding results show that the proposed machine is promising for application to electric vehicles.**

***Index Terms*—Brushless machine, electric vehicles, finite-element analysis, permanent magnet.**

I. Introduction

With ever-increasing concerns about environmental protection and energy conservation, the use of electric vehicles (EVs) for road transportation is becoming increasingly attractive. To enable EVs to directly compete with gasoline vehicles, the EV motor aims to pursue high efficiency, high power density, high controllability, wide speed range, and maintenance-free operation [1]. In order to pursue these goals, the doubly salient permanent magnet (DSPM) machine has been proposed which incorporates both the advantages of PM brushless and switched reluctance (SR) machines [2], [3]. However, it still suffers from the drawbacks of high PM material cost and uncontrollable PM flux. To alleviate these problems, a stator doubly fed doubly salient (SDFDS) machine topology has been proposed [4], which replaces the PM material by a dc field winding to facilitate flux weakening for constant power operation. However, this topology inevitably needs a high field winding magnetomotive force (MMF) to realize the desired flux weakening, hence degrading its electric loading and also its power density.

In this paper, a novel SDFDS-PM brushless machine topology is proposed, which not only reduces both PM material and field winding MMF significantly, but also offers a distinct advantage of wide constant power operation range (namely, up to four times the base speed), which is very important for EV application.

Manuscript received December 27, 2002. This work was supported by the Research Grants Council of the Hong Kong Special Administrative Region, China, under Grant HKU 7035/01E.

K. T. Chau and Y. Wang are with the Department of Electrical and Electronic Engineering, The University of Hong Kong, Hong Kong (e-mail: ktchau@eee.hku.hk; ywang@eee.hku.hk).

J. Z. Jiang is with the School of Automation, Shanghai University, Shanghai, China (e-mail: jzhjiang@yc.shu.edu.cn).

Digital Object Identifier 10.1109/TMAG.2003.816722

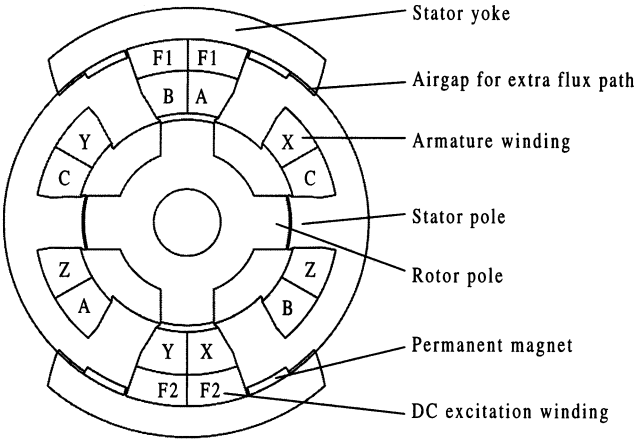

Fig. 1. Proposed machine topology.

II. Machine Topology

Fig. 1 shows the proposed topology, which is a three-phase 6/4-pole (six stator poles and four rotor poles) SDFDS-PM machine. It consists of two types of stator windings, a three-phase armature winding and a dc field winding. The three-phase armature winding operates like that for a DSPM machine [3], whereas the dc field winding not only works as an electromagnet but also as a tool for flux weakening and/or efficiency optimization. Notice that flux weakening operation is necessary for high-speed EV cruising, whereas efficiency optimizing control is essential for long EV driving range.

The novelty of this topology is an extra flux path in shunt with each PM pole. If the field winding MMF reinforces the PM MMF, this extra flux path will assist the effect of flux strengthening. On the other hand, if the field winding MMF opposes the PM MMF, this extra flux path will favor the PM flux leakage, hence amplifying the effect of flux weakening.

III. Principle of Operation

Under the assumptions that the fringing effect is negligible and the permeability of the iron core is infinite, a linear variation of flux linkage Φ results where the maximum value $\Phi_{\max}$ occurs at the alignment between the rotor pole and the stator pole, whereas the minimum value $\Phi_{\min}$ occurs at their nonalignment. When Φ is increasing, an armature current i with a positive value I_m is applied to the phase winding, hence producing a positive torque. Similarly, when Φ is decreasing, a negative current $-I_m$ is applied to the winding so that a positive torque is also produced. Thus, two possible torque producing zones are fully utilized. The corresponding theoretical waveforms of Φ and i with respect to the rotor position θ are shown in Fig. 2.

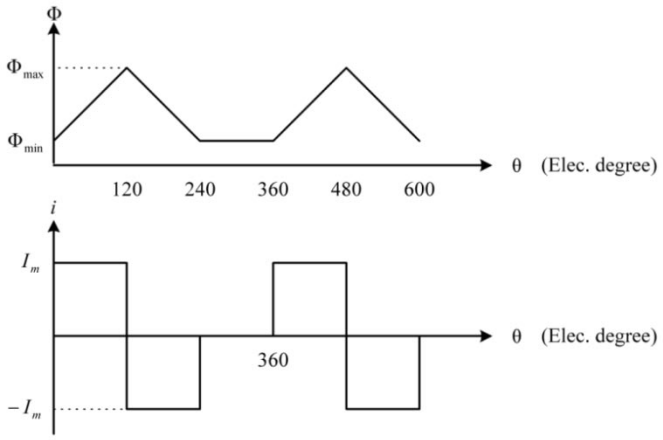

Fig. 2. Theoretical flux and current waveforms.

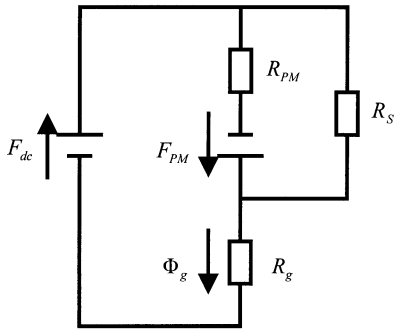

Fig. 3. Equivalent magnetic circuit at no-load.

Furthermore, the induced back EMF E at no-load can readily be deduced

$$E = N\,\frac{d\Phi}{d\theta}\,\omega_r \approx N\,\frac{\Delta\Phi}{\Delta\theta}\,\omega_r \tag{1}$$

where N is the number of turns in series of each phase winding, $\Delta\Phi$ is the difference between $\Phi_{\max}$ and $\Phi_{\min}$, $\Delta\theta$ is the angular difference between the rotor positions of $\Phi_{\max}$ and $\Phi_{\min}$, and ω_r is the angular rotor speed.

IV. Magnetic Circuit Analysis

As mentioned, the novelty of the proposed machine topology is the use of an extra flux path in shunt with each PM pole. In order to illustrate its merit, an equivalent magnetic circuit model is used for analysis.

Fig. 3 shows the equivalent magnetic circuit of the proposed machine at no-load, namely the armature current is set to zero. Based on this circuit, the airgap flux Φ_g can be expressed as

$$\Phi_g = \frac{F_{dc}\,(R_S + R_{PM}) + F_{PM}R_S}{R_S R_g + R_{PM}R_g + R_S R_{PM}} \tag{2}$$

where F_{dc} is the dc field winding excitation MMF, F_{PM} is the PM excitation MMF, R_{PM} is the reluctance of the PM pole, R_S is the reluctance of extra flux path, and R_g is the reluctance of the airgap. When there is no field winding excitation, $F_{dc} = 0$ so that the corresponding airgap flux is given by

$$\Phi_{g0} = \frac{F_{PM}R_S}{R_S R_g + R_{PM}R_g + R_S R_{PM}}. \tag{3}$$

When a positive field winding excitation is applied, $F_{dc} = F_{dc+}$ so that the corresponding airgap flux is given by

$$\Phi_{g+} = \frac{F_{dc+}\,(R_S + R_{PM}) + F_{PM}R_S}{R_S R_g + R_{PM}R_g + R_S R_{PM}}. \tag{4}$$

Similarly, when a negative field winding excitation is applied, $F_{dc} = F_{dc-}$ so that the corresponding airgap flux is given by

$$\Phi_{g-} = \frac{F_{dc-}\,(R_S + R_{PM}) + F_{PM}R_S}{R_S R_g + R_{PM}R_g + R_S R_{PM}}. \tag{5}$$

With (3) and (4), (5) yields

$$F_{dc+} = \frac{\frac{\Phi_{g+}}{\Phi_{g0}} - 1}{\frac{R_{PM}}{R_S} + 1}\,F_{PM}. \tag{6}$$

Similarly, by use of (3) and (5), we obtain

$$F_{dc-} = \frac{1 - \frac{\Phi_{g-}}{\Phi_{g0}}}{\frac{R_{PM}}{R_S} + 1}\,F_{PM}. \tag{7}$$

When selecting $(R_S/R_{PM}) = 1/3$, $(\Phi_{g+}/\Phi_{g0}) = 2$ and $(\Phi_{g-}/\Phi_{g0}) = 1/2$, (6) and (7) can be rewritten as

$$F_{dc+} = \frac{F_{PM}}{4} \tag{8}$$

$$F_{dc-} = \frac{F_{PM}}{8}. \tag{9}$$

It illustrates that a quadruple change in Φ_g, namely $(\Phi_{g+}/\Phi_{g-}) = 4$, needs only a small change in F_{dc}, namely 25% of F_{PM} during flux strengthening, and 12.5% of F_{PM} during flux weakening. Notice that the amplifying effect of F_{dc} during flux weakening is particularly important when the machine needs to operate at high speeds for EV cruising.

TABLE I
Design Data

Rated voltage	48 V
Rated current	6.5 A
Number of phases	3
Number of stator poles	6
Number of rotor poles	4
Number of turns per phase	64×2
Stator outer diameter	166.0 mm
Stator inner diameter	81.2 mm
Rotor outer diameter	80.0 mm
Rotor inner diameter	26.0 mm
Stack length	80.0 mm

V. Machine Performance

In order to assess the performance of the proposed machine while taking into account its magnetic saturation, leakage flux and armature reaction, finite-element analysis is applied to a newly designed prototype as listed in Table I. Fig. 4 shows the

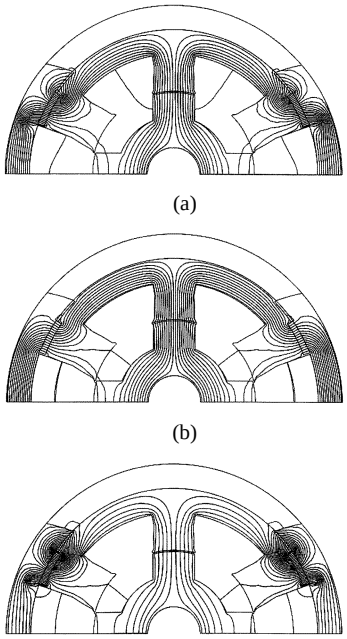

Fig. 4. Flux distributions at different dc excitations: (a) no excitation, (b) flux strengthening, and (c) flux weakening.

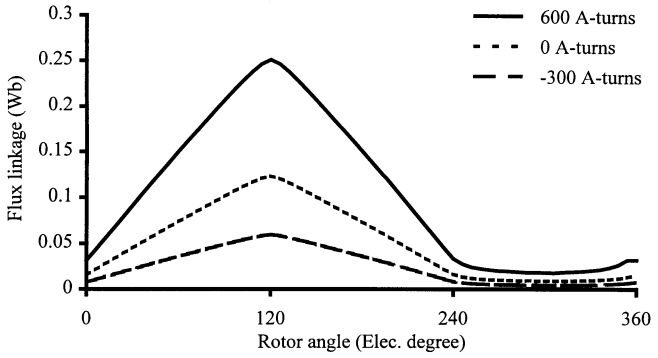

Fig. 5. Flux linkages at different dc excitations.

flux distributions of the proposed machine under no excitation with $F_{dc} = 0$, flux strengthening with $F_{dc} = 600$ A-turns, and flux weakening with $F_{dc} = -300$ A-turns, respectively. Particularly, Fig. 4(c) shows that the extra flux path can significantly favor the PM flux leakage, hence amplifying the effect of flux weakening, which agrees with the previous finding resulted from magnetic circuit analysis.

When the machine operates at no-load and runs at constant speed, the corresponding flux linkages with respect to the rotor position under different dc excitations, namely 600, 0, and -300 A-turns, are simulated as shown in Fig. 5. It can be found that both flux strengthening and flux weakening can be successfully achieved by control of the dc field current. Also, the pattern of these simulated flux linkages closely agrees with the theoretical one shown in Fig. 2.

When the machine operates at rated load, namely the armature current is 6.5 A, the corresponding armature reaction causes inevitable distortion of the main flux. Nevertheless, due to the large reluctance of the armature flux path, this armature reaction and its effect on the speed range are insignificant.

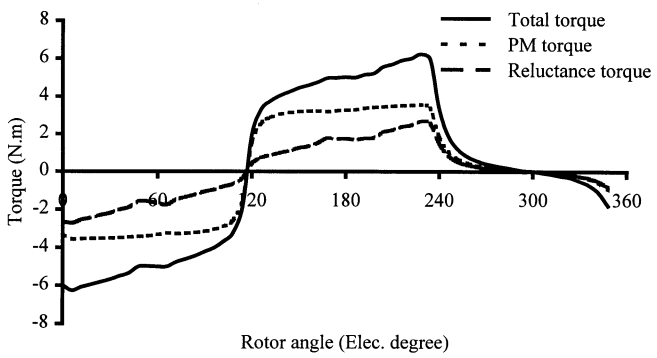

Fig. 6. Total torque and its components.

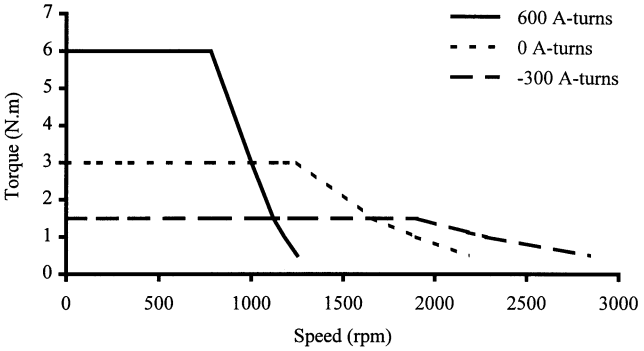

Fig. 7. Torque–speed characteristics at different dc excitations.

By application of the Maxwell tensor method, the developed torque with respect to the rotor position in the absence of dc excitation can be simulated as shown in Fig. 6. It should be noted that the total torque consists of two components, namely the PM torque and the reluctance torque. Furthermore, the torque–speed characteristics of the proposed machine under different dc excitations are simulated as shown in Fig. 7. It can be found that the speed range can be significantly widened to four times the base speed.

VI. Conclusion

A novel SDFDS-PM brushless machine has been proposed and analyzed. The novelty of this machine is addition of an extra flux path in shunt with each PM pole, hence amplifying the effect of flux weakening for constant power operation. Thus, the proposed machine not only offers the advantages of a DSPM machine, but also a very wide speed range which is essential for EV application.

References

[1] C. C. Chan and K. T. Chau, *Modern Electric Vehicle Technology*. London, U.K.: Oxford Univ. Press, 2001, pp. 67–83.

[2] Y. Liao, F. Liang, and T. A. Lipo, "A novel permanent magnet motor with doubly salient structure," *IEEE Trans. Ind. Applicat.*, vol. 31, pp. 1059–1078, Sept./Oct. 1995.

[3] M. Cheng, K. T. Chau, and C. C. Chan, "Design and analysis of a new doubly salient permanent magnet motor," *IEEE Trans. Magn.*, vol. 37, pp. 3012–3020, July 2001.

[4] K. T. Chau, M. Cheng, and C. C. Chan, "Nonlinear magnetic circuit analysis for a novel stator-doubly-fed doubly-salient machine," *IEEE Trans. Magn.*, vol. 38, pp. 2382–2384, Sept. 2002.